

Joint Radar-Communications Performance Bounds:

Data versus Estimation Information Rates

by

Alex Chiriyath

A Thesis Presented in Partial Fulfillment
of the Requirement for the Degree
Master of Science

Approved July 2014 by the
Graduate Supervisory Committee:

Daniel W. Bliss, Chair
Oliver Kosut
Visar Berisha

ARIZONA STATE UNIVERSITY

August 2014

ABSTRACT

The problem of cooperative radar and communications signaling is investigated. Each system typically considers the other system a source of interference. Consequently, the tradition is to have them operate in orthogonal frequency bands. By considering the radar and communications operations to be a single joint system, performance bounds on a receiver that observes communications and radar return in the same frequency allocation are derived. Bounds in performance of the joint system is measured in terms of data information rate for communications and radar estimation information rate for the radar. Inner bounds on performance are constructed.

DEDICATION

To my parents

ACKNOWLEDGEMENTS

I would like to take this opportunity to thank a few people who's knowledge and assistance have been invaluable to me. First and foremost, I would like to extend my gratitude to my advisor Professor Dan Bliss for mentoring me and providing invaluable insight at every stage of my research.

I would also like to thank Professors Oliver Kosut and Visar Berisha for taking the time to be members of my committee, and sharing their knowledge and expertise with me.

I would also like to thank Bryan Paul for his valuable comments.

Last but not the least, I would like to thank my friends and family, especially my parents, for their constant love and support.

This work was sponsored by DARPA under the SSPARC program. The views expressed are those of the author and do not reflect the official policy or position of the Department of Defense or the U.S. Government.

TABLE OF CONTENTS

	Page
LIST OF TABLES	vi
LIST OF FIGURES	vii
CHAPTER	
1 INTRODUCTION	1
1.1 Background	1
1.2 Contributions	4
1.3 Thesis Organization	6
2 JOINT RADAR-COMMUNICATIONS CHANNEL MODEL	7
2.1 Radar Return Signal Model	10
2.2 Communications Signal with Predicted Radar Return Suppressed ..	12
3 CRAMER-RAO LOWER BOUND FOR TIME-DELAY ESTIMATION .	14
4 RADAR ESTIMATION INFORMATION RATE	15
5 MULTIPLE-ACCESS COMMUNICATIONS PERFORMANCE BOUND	17
6 PERFORMANCE BOUNDS OF A JOINT RADAR-COMMUNICATIONS SYSTEM	19
6.1 Isolated Sub-band Inner Bound	20
6.2 Successive Interference Cancellation (SIC) Inner Bound	21
6.3 Communications Water-filling Inner Bound	22
6.4 Optimal Fisher Information Inner Bound	26
6.5 Examples	31
7 CONCLUSION	40
7.1 Summary	40
7.2 Future Research	42

CHAPTER	Page
REFERENCES	43
APPENDIX	
A DERIVATION OF CRAMER-RAO LOWER BOUND FOR TIME-DELAY ESTIMATION	47
B DERIVATION OF REDUCED FISHER INFORMATION FOR TIME-DELAY ESTIMATION FROM FISHER INFORMATION MATRIX FOR JOINT AMPLITUDE AND TIME-DELAY ESTIMATION	50

LIST OF TABLES

Table	Page
2.1 Survey of Notation	8
6.1 Parameters for Example Performance Bound #1	33
6.2 Parameters for Example Performance Bound #2	36
6.3 Parameters for Example Performance Bound #3	38

LIST OF FIGURES

Figure	Page
1.1 Joint Radar-Communications System	6
5.1 Pentagon containing Communications Multiple-Access Achievable Rate Region.	18
6.1 Receiver Block Diagram for SIC Scenario	21
6.2 Receiver Block Diagram for Communications Only and Mixed Use Sub- bands	23
6.3 Receiver Block Diagram for Radar Only and Mixed Use Sub-bands ...	26
6.4 Power distribution vs. (α) for Optimal Fisher Information Bound.	34
6.5 Data Rate and Estimation Rate Bounds for Parameters in Table 6.1. .	35
6.6 Data Rate and Estimation Rate Bounds for Parameters in Table 6.2. .	37
6.7 Data Rate and Estimation Rate Bounds for Parameters in Table 6.3. .	39

Chapter 1

INTRODUCTION

There is an ever increasing demand for spectrum and given the limit on resources, communications and radar are forced to share bandwidth. This causes inter-system interference and can degrade the performance of both systems. The standard solution is to separate (temporally, spatially or spectrally) the radar and communications systems. In this thesis, we do not require this separation, and we explore the fundamental radar and communications coexistence performance bounds. An important contribution that enables this exploration is the parameter of estimation information rate.

1.1 Background

In this thesis we reformulate and extend the performance bounds introduced in [1]. It is worth noting that in our efforts presented here, we focus on the radar estimation performance rather than radar detection considered in [2, 3, 4, 5, 6, 7, 8]. To be more specific, in our work, we have focused on the estimation of a target parameter, time delay or target range, from the received target return and the performance of the radar system is measured in terms of the estimation rate.

The work presented in [2, 3, 4, 5] investigated the application of information theory to improve radar system performance. It was in these works that the idea that signal-to-noise ratio (SNR) does not measure information is introduced. At the time, it was generally assumed that the higher the output SNR, the better the detection performance of a radar system. Hence, most radar systems or waveforms were designed to maximize the output SNR; however, this simple formulation misses

some of the subtleties. The primary focus of these works is to dispel such a simplistic interpretation by using information theory to formulate a new type of receiver, the *a posteriori* radar receiver, that does not try and maximize output SNR but attempts to maximize the quantity of information, given by the *a posteriori* distribution of a target parameter.

In [6], the problem of designing optimal waveforms for the cases of detection and target information extraction are considered. In the problem of target information extraction, the radar waveform is designed so as to maximize the mutual information between the target parameter of interest and the measurements obtained from the receiver. However, target parameter estimation (in the traditional sense) is never explicitly discussed, and the radar system performance is measured in terms of target classification ability or average measurement error.

In [7, 8], the theory of matched illumination, the process of optimizing the pulse shape of the radar waveform (finite duration and finite energy) and the impulse response of the receiver, is used to design a target detection system that maximizes the target SNR (which corresponds to maximizing the probability of detection in gaussian noise and interference).

Current research has investigated the benefits of using methods similar to cooperative sensing to solve the problem of radar and communications co-existence [9, 10]. Radar nodes that employ some form of cooperative sensing have shown an improvement when compared to traditional nodes that did not employ cooperative sensing. In [9] four regions of coexistence are defined between radar and communication systems which are separated based on whether the two systems interfere with each other and if this interference is detectable by either system. These regions are defined based on a set of INR/SNR thresholds and probability of interference/detection thresholds. The non-detectable/non-interfering region is the worst case region and the system

parameters should be chosen in such a way so as to make this region of coexistence as small as possible. Simple algorithms can be developed for the other regions. It is then shown that coexistence between radar and communications is feasible for radar nodes without cooperative sensing only when subject to stringent interference restrictions, low radar transmit power and among other constraints. However, among radar nodes that utilize cooperative sensing, coexistence is not subject to such stringent constraints. Furthermore radar nodes with cooperative sensing demonstrate an improvement in performance (especially if the nodes are spaced far apart, ensuring that the channel correlation between nodes is low) in terms of detection probability, detection range etc. Another approach is employed in [10] wherein the surveillance space of the radar system is divided into sectors and priorities are assigned to all radar and communication systems that want to transmit in each sector. The priorities are determined using fuzzy logic. The criteria used to assign these priorities include target separation, SNR, clutter etc. Bandwidth is allocated or 'shared' based on these priorities by performing multi-objective optimization.

Some other techniques such as interference mitigation [11], precoding or spatial separation [12] or waveform shaping [13] allow both radar and communications to share the spectrum and coexist. In [13], waveform shaping is done by projecting radar waveforms onto the null space of the interference channel matrix, which ensures that there is minimal interference on the communications system from the radar system. The interference channel matrix can be extracted from the complete channel matrix. The channel is assumed to be reciprocal (thus making it easier to estimate the channel matrix) and the radar system is assumed to be a colocated MIMO radar in which each antenna transmit mutually orthogonal waveforms. The channel matrix between the primary and secondary user is estimated by the secondary user and either system can be considered as the primary user. Once the channel matrix is estimated and the

null space of the interference channel matrix is calculated, the original radar waveform (any radar waveform) is then projected onto the null space and the resultant waveform is transmitted. It is then shown that such a radar system is able to perform at levels comparable to a case where null space projections on radar signals are not done and the radar system has no interference.

Radar systems based on communication systems, where radar systems use OFDM or DSSS signals as radar illumination signals, have also been considered [14, 15, 16, 17]. In [16], the radar system along with the communication system uses OFDM waveforms for transmission and algorithms are presented to assign OFDM sub-carriers to each system in such a way so as to optimize channel capacity for the communication system and the target detection performance (Mahalanobis distance [18]) for the radar system. The first algorithm is a low-complexity algorithm that assigns sub-carriers to each system such that the channel capacity and target detection performance are optimized separately while the second algorithm jointly optimizes the channel capacity and target detection performance.

Similarly, communication systems using radar illumination signals like linear frequency modulation (LFM) chirp waveforms as modulation signals to transmit data have been developed [19]. It has been shown in [19] that such a modulation scheme when used with a radar system shows good system performance in terms of bit error rate (for communications) and false-alarm rate (for radar). Signal sharing, a method in which both radar and communication systems utilize the same waveform has also been applied to the radar and communications coexistence problem [20, 21, 22].

1.2 Contributions

We consider the joint radar-communications receiver to be a radar node that can act as a communications relay as well. This means that the receiver can simultane-

ously estimate the radar target parameters from the radar return and decode a communications signal. This functioning of such a receiver is shown in Figure 1.1. In this thesis, we develop a new approach for producing joint radar-communications performance bounds. The joint radar-communications system decodes the communication signal jointly with the estimation of the radar channel. The principle contributions of this thesis are that we:

- Develop novel joint receiver formulation analogous to communication multiple access channel.
- Develop radar estimation rate, a metric analogous to data information rate.
- Derive the isolated sub-band inner bound.
- Derive the successive interference cancellation inner bound.
- Derive the communications water-filling inner bound.
- Derive the optimal fisher information inner bound.

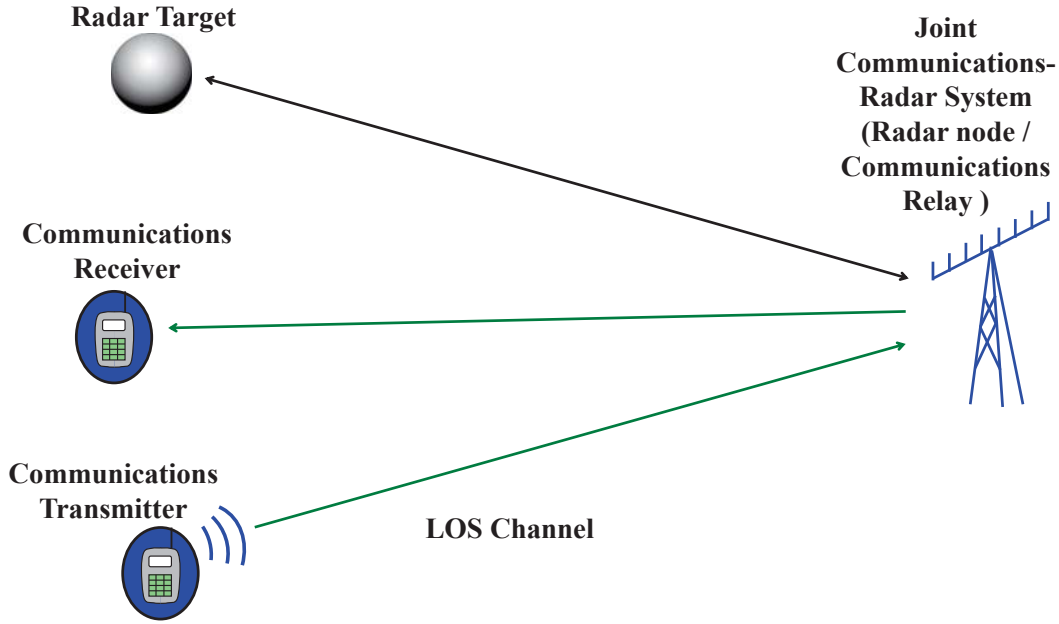


Figure 1.1: Joint Radar-Communications System

1.3 Thesis Organization

This thesis is organized as follows. In Chapter 2, we present the channel and signal model for a joint radar-communications system that will be employed in this thesis. We also introduce the idea of a observed signal with a predicted radar return signal suppressed. In Chapter 3, we present the Cramer-Rao lower bound on time-delay estimation for a joint radar-communications system considered in this thesis. In Chapter 4, we develop the radar estimation information rate. The estimation information rate is the metric which we will use to measure performance of the radar system. In Chapter 5, we present the multiple access communications performance bound as an analogy to the joint radar-communications system. In Chapter 6, we develop several inner bounds on the performance of the joint radar-communications system by considering various scenarios and developing estimation and data rates for the radar and communications systems respectively. Finally, in Chapter 7, we present a summary of results obtained in this thesis and avenues for future research.

JOINT RADAR-COMMUNICATIONS CHANNEL MODEL

In this chapter, we consider the joint radar-communications system received signal, $z(t)$, for a multiple-access communications and radar return channel. We present a table of significant notation that will be employed in this thesis in Table 2.1. We make the following assumptions:

- Target cross-section σ is nuisance parameter.
- Target cross-section is estimated well.
- Targets well separated.
- Residual of unpredicted radar return is modeled well by a Gaussian distribution before pulse compression.
- Target range known up to some Gaussian random process variation which is within one over the bandwidth.

We consider only the portion of time during which the radar return overlaps with the communications signal. For the sake of simplicity we focus on range estimation only, as opposed to range and amplitude estimation. The joint system receiver will attempt to suppress the radar return using the predicted target range and then proceed to decode the communications signal as shown in [1].

Table 2.1: Survey of Notation

Variable	Description
$\langle \cdot \rangle$	Expectation
θ	Estimation Parameters
$s(\theta; z(t))$	Score function of $z(t)$ with respect to θ
B	Bandwidth of the System
$z(t)$	Observed signal including radar and communications
$\tilde{z}_{\text{com}}(t)$	Observed signal with predicted radar return removed
$x(t)$	Unit-variance transmitted radar signal
P_{rad}	Radar power
τ_m	Time delay to m^{th} target
$\tau_m^{(k)}$	k^{th} observation of delay for m^{th} target
$\tau_{m,\text{pre}}$	Predicted time delay to m^{th} target
a_m	Complex combined antenna, cross-section, and propagation gain for m^{th} target
T	Radar pulse duration
N	Number of targets
δ	Radar duty factor

Continued on next page

Table 2.1 – *Continued from previous page*

Variable	Description
$r(t)$	Transmitted communication signal with variance σ_{noise}^2
P_{com}	Total communications power
b	Communications propagation loss (amplitude)
$n(t)$	Receiver thermal noise
σ_{noise}^2	Thermal noise power
k_B	Boltzmann constant
T_{temp}	Absolute Temperature
$n_{\text{int+n}}$	Interference plus noise for communications receiver
θ	Set of nonspecific system and target parameters
B_{rms}	Root-mean-squared radar bandwidth
γ	Radar spectral shape parameter
B_{com}	Communications only sub-band
B_{rad}	Radar only sub-band
B_{mix}	Mixed radar and communications sub-band
α	Fraction of bandwidth for communications only

Continued on next page

Table 2.1 – *Continued from previous page*

Variable	Description
β	Power fraction used by communications-only sub-band
ρ_{RO}	Power Spectral Density used by radar only sub-band
ρ_{MU}	Power Spectral Density used by mixed use sub-band
μ_{com}	Channel of communications-only sub-band
μ_{mix}	Channel of mixed use sub-band
$\text{SNR}_{\text{radar}}$	Signal-to-noise-ratio of radar estimator

2.1 Radar Return Signal Model

Unless stated otherwise, we always assume that all signals are in complex-baseband. While this may not seem pertinent now, this becomes convenient later, when computing the information rates (estimation and data) of both radar and communication systems [23].

For N targets, the observed radar return $z_{\text{rad}}(t)$ without any communications signal interference, is given by

$$z_{\text{rad}}(t) = \sum_{m=1}^N a_m \sqrt{P_{\text{rad}}} x(t - \tau_m) + n(t). \quad (2.1)$$

Additionally, the observed signal at the receiver $z(t)$ in the presence of a communi-

cations signal is given by

$$z(t) = b \sqrt{P_{\text{com}}} r(t) + \sqrt{P_{\text{rad}}} \sum_{m=1}^N a_m x(t - \tau_m) + n(t). \quad (2.2)$$

The zero-mean thermal noise is drawn from a complex Gaussian distribution with variance $\sigma_{\text{noise}}^2 = k_B T_{\text{temp}} B$, where k_B is the Boltzmann constant, T_{temp} is the absolute temperature, and B is the full bandwidth. Similar developments can be found for amplitude estimation. A reasonable time-delay estimator (particularly if targets are well separated) is the correlation estimator given by

$$\hat{\tau}_m = \operatorname{argmax}_{\tau_m} \int dt z(t) x^*(t - \tau_m). \quad (2.3)$$

As stated above, because we assume we are tracking the target, we have some knowledge of the target's range (based upon prior observations), up to some range fluctuation in the return due to an underlying target random process. This range fluctuation is interpreted as a fluctuation in time and this delay fluctuation is modeled by a Gaussian distribution $n_{\tau, \text{proc}}$. During the k^{th} observation, the delay for the m^{th} target will be given by,

$$\begin{aligned} \tau_m^{(k)} &= \tau_{m, \text{pre}}^{(k)} + n_{\tau, \text{proc}} \\ \tau_{m, \text{pre}}^{(k)} &= f(k; T_{\text{pri}}, \boldsymbol{\theta}). \end{aligned} \quad (2.4)$$

The function $f(k; T_{\text{pri}}, \boldsymbol{\theta})$ is a prediction function which depends on T_{pri} , the pulse repetition interval, and a set of nonspecific system and target parameters, $\boldsymbol{\theta}$. The variance of the range fluctuation process is given by

$$\sigma_{\tau, \text{proc}}^2 = \langle \|n_{\tau, \text{proc}}\|^2 \rangle = \left\langle \|\tau_m^{(k)} - f(k; T_{\text{pri}}, \boldsymbol{\theta})\|^2 \right\rangle. \quad (2.5)$$

2.2 Communications Signal with Predicted Radar Return Suppressed

In order to improve performance of the communications system, we try to mitigate unnecessary interference caused by the presence of the radar signal by using the predicted target range to generate a predicted radar return and subtracting it from the received signal at the receiver.

For N targets, the received signal at the communications receiver with the predicted radar return suppressed is given by

$$\begin{aligned} \tilde{z}_{\text{com}}(t) &= \sqrt{P_{\text{com}}} b r(t) + n(t) \\ &+ \sqrt{P_{\text{rad}}} \sum_{m=1}^N a_m [x(t - \tau_m) - x(t - \tau_{m,\text{pre}})]. \end{aligned} \quad (2.6)$$

Note: we have assumed here that the estimated amplitude is equal to the actual amplitude i.e. $\hat{a}_m = a_m$. This approach is only useful if the error in delay is smaller than $1/B$. For small fluctuations in delay, we can replace the difference between the actual and predicted radar return waveforms with a derivative,

$$\begin{aligned} &x(t - \tau_m) - x(t - \tau_{m,\text{pre}}) \\ &= x(t - \tau_m) - x(t - \tau_m - n_{\tau,\text{proc}}) \\ &\approx \frac{\partial x(t - \tau_m)}{\partial t} n_{\tau,\text{proc}}. \end{aligned} \quad (2.7)$$

The signal observed by the communications receiver is then given by

$$\begin{aligned} \tilde{z}_{\text{com}}(t) &\approx \sqrt{P_{\text{com}}} b r(t) + n(t) \\ &+ \sqrt{P_{\text{rad}}} \sum_{m=1}^N a_m \frac{\partial x(t - \tau_m)}{\partial t} n_{\tau,\text{proc}}. \end{aligned} \quad (2.8)$$

The interference plus noise from the communications system's point of view is given

by

$$\begin{aligned}
n_{\text{int+n}} &= \sqrt{P_{\text{rad}}} \sum_{m=1}^N a_m [x(t-\tau_m) - x(t-\tau_{m,\text{pre}})] + n(t) \\
&\approx \sqrt{P_{\text{rad}}} \left(\sum_{m=1}^N a_m \frac{\partial x(t-\tau_m)}{\partial t} n_{\tau,\text{proc}} \right) + n(t) \\
\sigma_{\text{int+n}}^2 &= \langle \|n_{\text{int+n}}\|^2 \rangle \\
&= P_{\text{rad}} \left(\sum_{m=1}^N \|a_m\|^2 (2\pi)^2 B_{\text{rms}}^2 \sigma_{\text{proc}}^2 \right) + \sigma_{\text{noise}}^2 \tag{2.9}
\end{aligned}$$

$$B_{\text{rms}} = \frac{\int df f^2 \|X(f)\|^2}{\int df \|X(f)\|^2}, \tag{2.10}$$

where B_{rms} comes from employing Parseval's theorem to convert $\partial x(t-\tau_m)/\partial t$ into the frequency domain and then using the differentiation property of the fourier transform [23]. B_{rms} is extracted from bandwidth B as follows

$$\gamma^2 B^2 = (2\pi)^2 B_{\text{rms}}^2, \tag{2.11}$$

where the value γ is the scaling constant between B and B_{rms} times 2π that is dependent upon the shape of the radar waveform's power spectral density. For a flat spectral shape, $\gamma^2 = (2\pi)^2/12$.

CRAMER-RAO LOWER BOUND FOR TIME-DELAY ESTIMATION

In this chapter, we will go over the Cramer-Rao lower bound on time-delay estimation on a SISO (single-input single-output) channel with circularly symmetric Gaussian noise [24]. We have gone over the derivation in more detail in Appendix A. The Cramer-Rao bound gives the best performance (in terms of variance of error) of an unbiased estimator.

We assume that the received signal of the time-delay estimator is given by

$$z(t) = a x(t - \tau) + n(t), \quad (3.1)$$

where $x(t)$ is the transmitted signal whose frequency representation, $X(f)$ has full bandwidth B , $x(t - \tau)$ is the delayed version of the transmitted signal, a is the combined radar cross-section, antenna and propagation gain and $n(t)$ is circularly symmetric Gaussian noise with zero mean and variance σ^2 .

Let $\theta = \tau$ be the parameter to be estimated. From equation (3.1), we see that $z(t) \sim \mathcal{CN}(x(t - \tau), \sigma^2)$ and has the following probability density function,

$$p(z(t); \theta) = \frac{1}{\pi\sigma^2} e^{-\frac{\|z(t) - a x(t - \tau)\|^2}{\sigma^2}}. \quad (3.2)$$

Eventually, we see that the Cramer-Rao lower bound for time delay estimation, $\sigma_{\tau; \text{est}}^2$ (as derived in Appendix A) is given by

$$\sigma_{\tau; \text{est}}^2 = J^{-1} = \left(\frac{1}{8\pi^2 B_{\text{rms}}^2 \text{ISNR}} \right) \quad (3.3)$$

where ISNR stands for integrated SNR. By centering the spectrum at an appropriate point(i.e. choosing the origin of the spectrum), we get the RMS bandwidth B_{rms} , given by Equation (2.10).

RADAR ESTIMATION INFORMATION RATE

In order to compare the performance of the radar and communications systems in terms of information rate, we need a metric analogous to data information rate for the communications system that can be used to measure the performance of the radar system. We consider this information rate by considering the entropy of a random parameter being estimated and the entropy of the estimation uncertainty of that parameter [1]. As an observation, if the targets are well separated, then each target estimation can be considered an independent information channel.

Motivated by the mutual information rate (or radar estimation rate) in terms of estimation entropy, random process entropy of the radar and bits per pulse repetition interval $T_{\text{pri}} = T/\delta$, the radar estimation information rate is bounded by

$$R_{\text{est}} \leq \sum_m \frac{h_{\tau,\text{rr}} - h_{\tau,\text{est}}}{T_{\text{pri}}}, \quad (4.1)$$

where $h_{\tau,\text{rr}}$ is the random process entropy and $h_{\tau,\text{est}}$ is the estimation entropy.

The random process entropy of the radar or the entropy of the process uncertainty plus estimation uncertainty, assuming that both are Gaussian, is given by [25, 23]

$$h_{\tau,\text{rr}} = \log_2[\pi e (\sigma_{\tau,\text{proc}}^2 + \sigma_{\tau,\text{est}}^2)]. \quad (4.2)$$

To find the estimation entropy, we find the delay estimation uncertainty for each target. Under the assumption of Gaussian estimation error, the resulting entropy of the error is given by

$$\begin{aligned} h_{\tau,\text{est}} &= \log_2[\pi e \sigma_{\tau,\text{est}}^2] \\ &= \log_2 \left[\pi e \frac{k_B T_{\text{temp}}}{2\gamma^2 B (TB) \|a_m\|^2 P_{\text{rad}}} \right], \end{aligned} \quad (4.3)$$

where the variance of delay estimation for the m^{th} target is given by Equation (3.3).

Finally, after putting it all together, we see that the radar estimation information rate is given by

$$\begin{aligned}
R_{\text{est}} &\leq \sum_m \frac{\delta}{T} \log_2 \left(1 + \frac{\sigma_{\tau, \text{proc}}^2}{\sigma_{\tau, \text{est}}^2} \right) \\
&= \sum_m B \log_2 \left[1 + \frac{2\sigma_{\tau, \text{proc}}^2 \gamma^2 B (TB) \|a_m\|^2 P_{\text{rad}}}{k_B T_{\text{temp}}} \right]^{\delta/(TB)} \\
&= \sum_m B \log_2 [1 + \text{SNR}_{m, \text{radar}}]^{\delta/(TB)} .
\end{aligned} \tag{4.4}$$

Note: the effective $\text{SNR}_{m, \text{radar}}$ is not a real signal to noise ratio, but it has a form reminiscent of the traditional SNR.

It is worth noting, that by employing this estimation entropy in the rate bound, it is assumed that the estimator achieves the Cramer-Rao performance. If the error variance is larger, then the rate bound is lowered.

MULTIPLE-ACCESS COMMUNICATIONS PERFORMANCE BOUND

We present the multiple-access communications system performance bound [25, 23] as motivation to develop inner bounds on the performance of a joint radar-communications system [1]. In this scenario, the channel propagation gain for the first communications system is given by a_1 and channel propagation gain for the second communications system is given by a_2 . The power of the first communications transmitter is denoted by P_1 and the power of the second communications transmitter is given by P_2 . Their corresponding rates are denoted R_1 and R_2 . Assuming that the noise variance is given by σ_{noise}^2 , the fundamental limits on rate are given by

$$\begin{aligned} R_1 &\leq \log_2 \left(1 + \frac{\|a_1\|^2 P_1}{\sigma_{\text{noise}}^2} \right) \\ R_2 &\leq \log_2 \left(1 + \frac{\|a_2\|^2 P_2}{\sigma_{\text{noise}}^2} \right) \\ R_1 + R_2 &\leq \log_2 \left(1 + \frac{\|a_1\|^2 P_1 + \|a_2\|^2 P_2}{\sigma_{\text{noise}}^2} \right) \end{aligned} \quad (5.1)$$

Vertices are found by jointly solving two bounds to get,

$$\{R_1, R_2\} = \left\{ \log_2 \left(1 + \frac{\|a_1\|^2 P_1}{1 + \|a_2\|^2 P_2} \right), \log_2 \left(1 + \frac{\|a_2\|^2 P_2}{\sigma_{\text{noise}}^2} \right) \right\},$$

and

$$\{R_1, R_2\} = \left\{ \log_2 \left(1 + \frac{\|a_1\|^2 P_1}{\sigma_{\text{noise}}^2} \right), \log_2 \left(1 + \frac{\|a_2\|^2 P_2}{1 + \|a_1\|^2 P_1} \right) \right\}.$$

The region that satisfies these theoretical bounds is depicted in Figure 5.1.

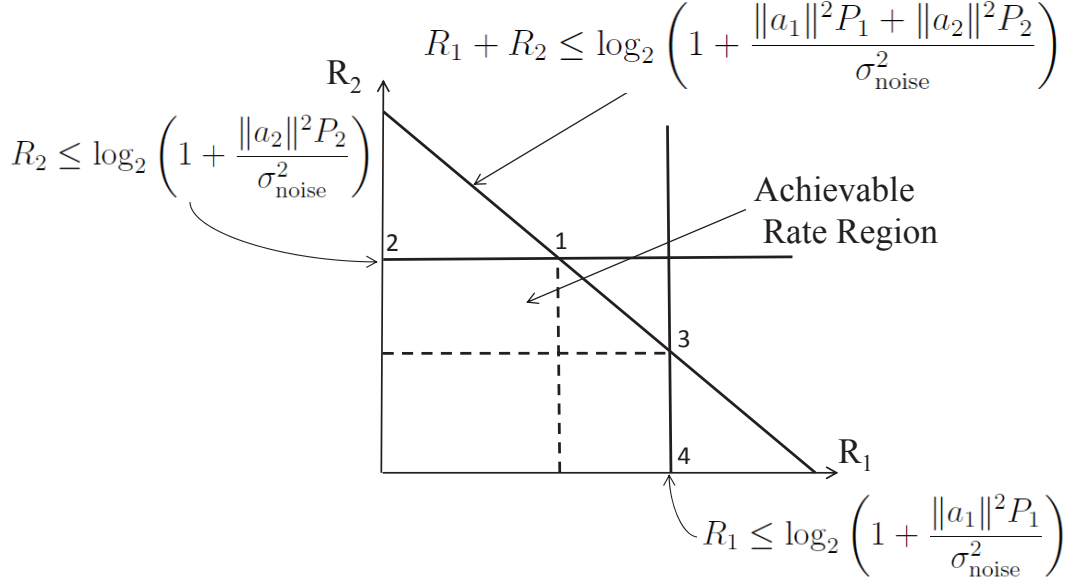


Figure 5.1: Pentagon containing Communications Multiple-Access Achievable Rate Region.

The achievable rate region is obtained by taking the convex hull [26] of the vertices 1-4. Depending on the amount of time each user occupies the channel, we can jump between vertex 1 and 3 along the convex hull. If user 1 utilizes the channel for a larger percentage of time, the closer we are to vertex 3 and vice versa. It is worth noting that there is no sense of the bits from user 1 are more or less important than the bits from user 2. The bound sets a joint limit that can be traversed depending on the percentage of time each user occupies the channel.

Since a radar signal is not derived from a countable dictionary, this violates the fundamental assumption of a communications signal and the bounds presented here can never be achieved by a joint communication-radar system. However, by employing an approach similar to the one discussed above, an outer bound on the performance of a joint radar-communications can be obtained.

PERFORMANCE BOUNDS OF A JOINT RADAR-COMMUNICATIONS
SYSTEM

In this chapter, we will derive inner bounds on the performance of the joint radar-communications system. As mentioned earlier, performance is measured in data information rate for the communications system and estimation information rate for the radar system. We consider a bound similar to the multiple-access communications performance bound derived in the previous chapter as an outer bound. We do not expect that the bound is achievable. We will also derive achievable inner bounds. The fundamental system performance limit lies between these achievable inner bounds and the outer bound. To find these inner bounds, we hypothesize an idealized receiver and determine the bounding rates. To simplify the discussion, we consider only a single target with delay τ and gain-propagation-cross-section product a^2 .

When deriving the bounds presented in this chapter, the radar pulse duration or T has always been fixed as constant. In some scenarios, this implies that the time-bandwidth product of the radar system will not be constant. In [1], a case was made for ensuring that the time-bandwidth product of the radar system would be fixed as constant which meant that the radar pulse duration would be constant. This would cause the duty-factor of the radar system δ to vary as well, which is not a desirable feature for radar systems. Furthermore, in some cases, a varying radar pulse duration would cause the radar pulse duration to exceed the pulse repetition interval of the radar system, i.e. $T > T_{\text{pri}}$, which would render the radar system unable to function correctly. It is for these reasons that the radar pulse duration has been fixed constant in all the scenarios presented in this chapter.

6.1 Isolated Sub-band Inner Bound

In this section, we derive an inner bound by considering a scenario in which we partition the total bandwidth into two sub-bands, one for radar only and the other for communications. Each system functions without any interference in their respective sub-band.

The bandwidth will be split between the two sub-bands according to some α such that,

$$B = B_{\text{rad}} + B_{\text{com}} \quad (6.1)$$

$$B_{\text{com}} = \alpha B$$

$$B_{\text{rad}} = (1 - \alpha) B.$$

The corresponding communication rate (for the communications only sub-band) is given by

$$\begin{aligned} R_{\text{com}} &\leq B_{\text{com}} \log_2 \left[1 + \frac{b^2 P_{\text{com}}}{k_B T_{\text{temp}} B_{\text{com}}} \right] \\ &\leq \alpha B \log_2 \left[1 + \frac{b^2 P_{\text{com}}}{k_B T_{\text{temp}} \alpha B} \right]. \end{aligned} \quad (6.2)$$

and the corresponding radar estimation rate is given by

$$\begin{aligned} R_{\text{est}} &\leq B_{\text{rad}} \log_2 \left(1 + \frac{2\sigma_{\text{proc}}^2 \gamma^2 B_{\text{rad}}^2 T \|a\|^2 P_{\text{rad}}}{k_B T_{\text{temp}}} \right)^{\delta/(TB_{\text{rad}})} \\ &= (1 - \alpha) B \log_2 (1 + \text{SNR}_{\text{radar}})^{\delta/([1-\alpha]TB)} \end{aligned} \quad (6.3)$$

$$\text{SNR}_{\text{radar}} = \frac{\sigma_{\text{proc}}^2 \gamma^2 (1 - \alpha) B ([1 - \alpha] TB) \|a\|^2 P_{\text{rad}}}{k_B T_{\text{temp}}}. \quad (6.4)$$

This inner rate bound follows the water-filling bound until the water-filling bound reaches the critical point (the transition between using one or both channels for communications) described by Equation (6.13). This is because before the critical

point is reached, both systems in the water-filling approach exist in isolated sub-bands and do not interfere with each other. Once the critical point has been reached, the water-filling approach starts allocating power to both sub bands, which causes the water-filling bound to deviate from the isolated sub-band bound.

6.2 Successive Interference Cancellation (SIC) Inner Bound

We consider a simple scenario in which the joint radar-communications system takes the received communications signal with suppressed predicted radar return and attempts to decode the communications signal. After the receiver has finished the decoding process, it can then remove the communications signal from the observed waveform and with some radar signal processing, we can obtain the original radar return signal free of any communications interference. The inner bound on performance derived through this scenario is called the SIC bound. The block diagram of the receiver considered in this scenario is shown in Figure 6.1.

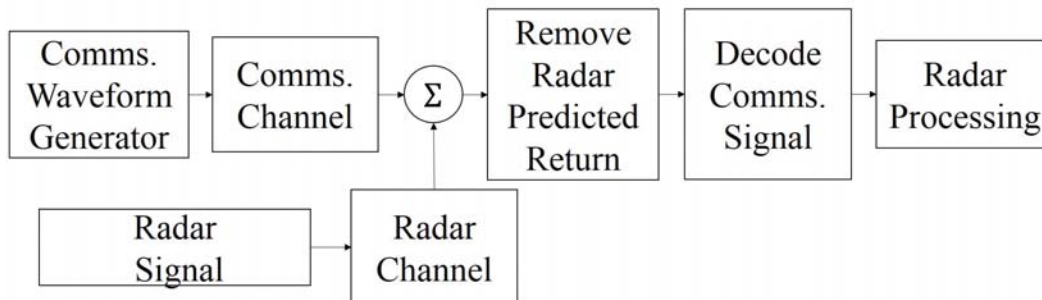


Figure 6.1: Receiver Block Diagram for SIC Scenario

If $R_{\text{est}} \approx 0$, it is as if the radar interference is not present and the communications system can operate at a data rate determined by the isolated communications bound,

$$\begin{aligned}
 R_{\text{com}} &\leq B \log_2 \left(1 + \frac{b^2 P_{\text{com}}}{\sigma_{\text{noise}}^2} \right) \\
 &= B \log_2 \left(1 + \frac{b^2 P_{\text{com}}}{k_B T_{\text{temp}} B} \right). \tag{6.5}
 \end{aligned}$$

If R_{com} is sufficiently low for a given transmit power, then as described above, the receiver can successfully decode the communications signal and remove it from the observed waveform, leaving just the radar return. Thus, the radar parameters, such as target range, can be estimated without corruption from any outside interference. This implies that from the communications receiver's perspective, it observes interference plus noise as described by Equation (2.9),

$$\begin{aligned} R_{\text{com}} &\leq B \log_2 \left[1 + \frac{b^2 P_{\text{com}}}{\sigma_{\text{int+n}}^2} \right] \\ &= B \log_2 \left[1 + \frac{b^2 P_{\text{com}}}{\|a\|^2 P_{\text{rad}} \gamma^2 B^2 \sigma_{\text{proc}}^2 + k_B T_{\text{temp}} B} \right], \end{aligned} \quad (6.6)$$

In this regime, the corresponding estimation rate bound R_{est} is given by Equation (5.1).

These two vertices correspond to the points 2 (associated with Equation (6.5)) and 3 (associated with Equations (6.6) and (5.1)) in Figure 5.1, assuming that R_1 is the estimation rate, and R_2 is the communications rate. An achievable rate lies within the quadrilateral constructed by constructing the convex hull between these points. This is the SIC inner bound.

6.3 Communications Water-filling Inner Bound

In this section, we consider a scenario in which the total bandwidth is split into two sub-bands, one sub-band for communications only and the other sub-band for both radar and communications. We use a water-filling approach to distribute the total communications power between the two bands [1]. Water-filling optimizes the power and rate allocation between multiple channels [25, 23]. The mixed use channel operates at the SIC rate vertex defined by Equations (5.1) and (6.6). The block diagram of the receiver considered in this scenario is shown in Figure 6.2.

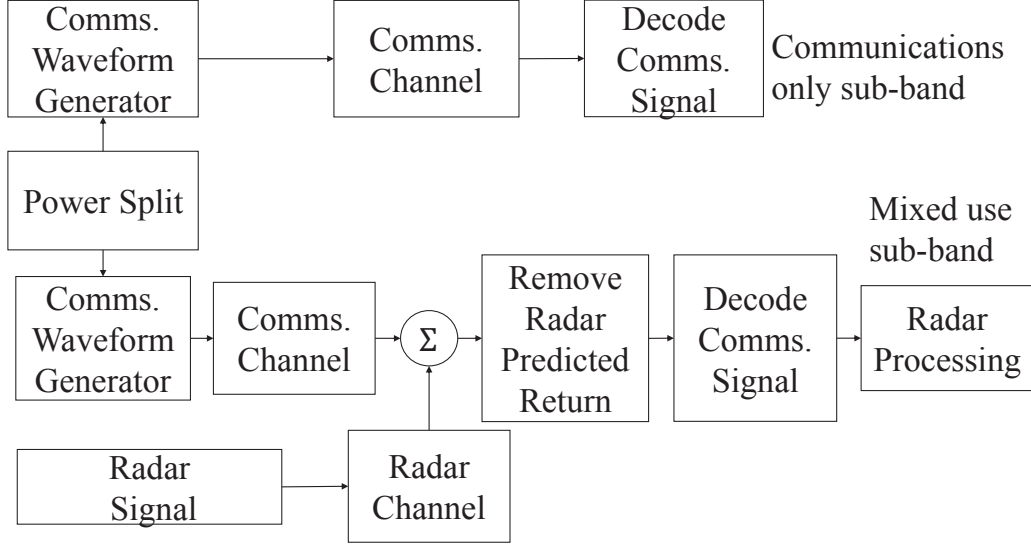


Figure 6.2: Receiver Block Diagram for Communications Only and Mixed Use Sub-bands

Given some α that defines the bandwidth separation,

$$B = B_{\text{com}} + B_{\text{mix}} \quad (6.7)$$

$$B_{\text{com}} = \alpha B$$

$$B_{\text{mix}} = (1 - \alpha) B,$$

then we optimize the power utilization, β ,

$$P_{\text{com}} = P_{\text{com,com}} + P_{\text{com,mix}} \quad (6.8)$$

$$P_{\text{com,com}} = \beta P_{\text{com}}$$

$$P_{\text{com,mix}} = (1 - \beta) P_{\text{com}}.$$

There are two effective channels

$$\mu_{\text{com}} = \frac{b^2}{k_B T_{\text{temp}} B_{\text{com}}} = \frac{b^2}{k_B T_{\text{temp}} \alpha B}, \quad (6.9)$$

for the communications only channel and

$$\begin{aligned}\mu_{\text{mix}} &= \frac{b^2}{\sigma_{\text{int+n}}^2} \\ &= \frac{b^2}{\|a\|^2 P_{\text{rad}} (1 - \alpha)^2 \gamma^2 B^2 \sigma_{\text{proc}}^2 + k_B T_{\text{temp}} (1 - \alpha) B}\end{aligned}\tag{6.10}$$

for the mixed use channel. The communications power is split between the two channels [25, 23],

$$\begin{aligned}P_{\text{com}} &= P_{\text{com,com}} + P_{\text{com,mix}} \\ &= \left(\alpha \nu - \frac{1}{\mu_{\text{com}}} \right)^+ + \left((1 - \alpha) \nu - \frac{1}{\mu_{\text{mix}}} \right)^+.\end{aligned}\tag{6.11}$$

The critical point (the transition between using one or both channels for communications) occurs when

$$\begin{aligned}(1 - \alpha) \nu - \frac{1}{\mu_{\text{mix}}} &= 0 \\ P_{\text{com}} &= \alpha \nu - \frac{1}{\mu_{\text{com}}},\end{aligned}\tag{6.12}$$

so both channels are used if

$$P_{\text{com}} \geq \frac{\alpha}{(1 - \alpha) \mu_{\text{mix}}} - \frac{1}{\mu_{\text{com}}}.\tag{6.13}$$

If the communications-only channel is used exclusively for communications, then $P_{\text{com}} = P_{\text{com,com}}$. If both channels are employed for communications then

$$\begin{aligned}P_{\text{com,com}} &= \alpha \nu - \frac{1}{\mu_{\text{com}}} \\ P_{\text{com,mix}} &= (1 - \alpha) \nu - \frac{1}{\mu_{\text{mix}}},\end{aligned}\tag{6.14}$$

and thus when Equation (6.13) is satisfied

$$\begin{aligned}P_{\text{com}} &= \alpha \nu - \frac{1}{\mu_{\text{com}}} + (1 - \alpha) \nu - \frac{1}{\mu_{\text{mix}}} \\ \nu &= \left(P_{\text{com}} + \frac{1}{\mu_{\text{com}}} + \frac{1}{\mu_{\text{mix}}} \right).\end{aligned}\tag{6.15}$$

The value of power fraction β is then given by

$$\begin{aligned}
\beta &= \frac{P_{\text{com,com}}}{P_{\text{com}}} \\
&= \frac{\alpha \nu - \frac{1}{\mu_{\text{com}}}}{P_{\text{com}}} \\
&= \frac{\alpha \left(P_{\text{com}} + \frac{1}{\mu_{\text{com}}} + \frac{1}{\mu_{\text{mix}}} \right) - \frac{1}{\mu_{\text{com}}}}{P_{\text{com}}} \\
&= \alpha + \frac{1}{P_{\text{com}}} \left(\frac{\alpha - 1}{\mu_{\text{com}}} + \frac{\alpha}{\mu_{\text{mix}}} \right); \\
&\text{when } P_{\text{com}} \geq \frac{\alpha}{(1 - \alpha) \mu_{\text{mix}}} - \frac{1}{\mu_{\text{com}}}. \tag{6.16}
\end{aligned}$$

The resulting communications rate bound in the communications-only sub-band is given by

$$\begin{aligned}
R_{\text{com,com}} &\leq B_{\text{com}} \log_2 \left[1 + \frac{P_{\text{com,com}} b^2}{k_B T_{\text{temp}} B_{\text{com}}} \right] \\
&\leq \alpha B \log_2 \left[1 + \frac{\beta P_{\text{com}} b^2}{k_B T_{\text{temp}} \alpha B} \right]. \tag{6.17}
\end{aligned}$$

The mixed use communications rate inner bound is given by

$$\begin{aligned}
R_{\text{com,mix}} &\leq B_{\text{mix}} \log_2 \left[1 + \frac{b^2 P_{\text{mix}}}{\sigma_{\text{int+n}}^2} \right] \\
&= (1 - \alpha) B \log_2 \left[1 + \frac{b^2 (1 - \beta) P_{\text{com}}}{\sigma_{\text{int+n}}^2} \right] \tag{6.18}
\end{aligned}$$

$$\sigma_{\text{int+n}}^2 = \|a\|^2 P_{\text{rad}} (1 - \alpha)^2 \gamma^2 B^2 \sigma_{\text{proc}}^2 + k_B T_{\text{temp}} (1 - \alpha) B.$$

The corresponding radar estimation rate inner bound is then given by

$$\begin{aligned}
R_{\text{est}} &\leq B_{\text{mix}} \\
&\log_2 \left(1 + \frac{2\sigma_{\text{proc}}^2 \gamma^2 B_{\text{mix}} (TB_{\text{mix}}) \|a\|^2 P_{\text{rad}}}{k_B T_{\text{temp}}} \right)^{\delta/(TB_{\text{mix}})} \\
&= (1 - \alpha) B \log_2 (1 + \text{SNR}_{\text{radar}})^{\delta/([1-\alpha]TB)} \tag{6.19}
\end{aligned}$$

$$\text{SNR}_{\text{radar}} = \frac{2\sigma_{\text{proc}}^2 \gamma^2 (1 - \alpha) B ([1 - \alpha] TB) \|a\|^2 P_{\text{rad}}}{k_B T_{\text{temp}}}. \tag{6.20}$$

6.4 Optimal Fisher Information Inner Bound

In this section, we construct another inner rate bound by considering an approach similar to the one utilized in the previous section. We split the total bandwidth into two sub-bands and distribute the radar power (or power spectral density) between the two sub-bands (instead of the communications power) in a way that minimizes the Cramer-Rao lower bound (or maximizes the Fisher information) on the variance of a time-delay estimator. Hence, we will have one channel that has radar only and the other channel will have both communications and radar. The block diagram of the receiver considered in this scenario is shown in Figure 6.3.

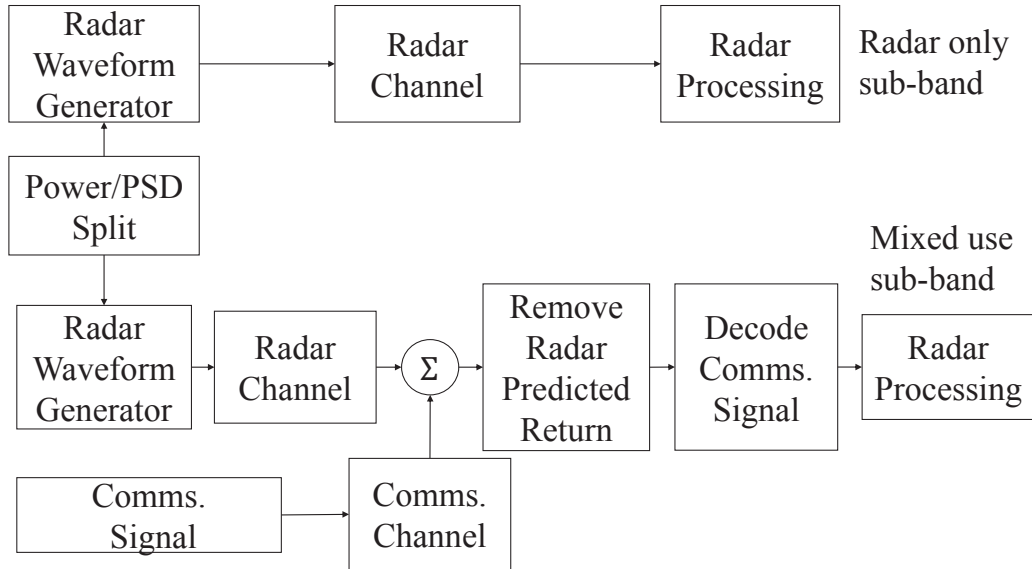


Figure 6.3: Receiver Block Diagram for Radar Only and Mixed Use Sub-bands

The bandwidth will be split between the two sub-bands according to some α such that,

$$B = B_{\text{rad}} + B_{\text{mix}} \quad (6.21)$$

$$B_{\text{rad}} = \alpha B$$

$$B_{\text{mix}} = (1 - \alpha) B,$$

and we will optimize the power spectral densities, ρ_{RO} and ρ_{MU} , utilized by the radar only and mixed use sub-bands respectively, to maximize the Fisher information, where

$$P_{\text{rad}} = P_{\text{rad,rad}} + P_{\text{rad,mix}} \quad (6.22)$$

$$\begin{aligned} P_{\text{rad,rad}} &= B_{\text{rad}} \rho_{\text{RO}} \\ &= \alpha B \rho_{\text{RO}} \end{aligned} \quad (6.23)$$

$$\begin{aligned} P_{\text{rad,mix}} &= B_{\text{mix}} \rho_{\text{MU}} \\ &= (1 - \alpha)B \rho_{\text{MU}}. \end{aligned} \quad (6.24)$$

We will have the following constraints on power and energy of the radar system in the two sub-channels,

$$P_{\text{rad}} = \alpha B \rho_{\text{RO}} + (1 - \alpha)B \rho_{\text{MU}} \quad (6.25)$$

$$E_{\text{rad}} = T P_{\text{rad}} = \alpha T B \rho_{\text{RO}} + (1 - \alpha) T B \rho_{\text{MU}}. \quad (6.26)$$

Now, consider a radar signal $x(t)$ with bandwidth B , whose frequency spectrum $X(f)$ is centered around $B_{\mathcal{O}}$. We assume that $X(f)$ is spectrally flat. We will now partition the frequency spectrum into two portions, $X_{\text{RO}}(f)$ and $X_{\text{MU}}(f)$ with bandwidths αB and $(1 - \alpha)B$ respectively, thereby creating two new signals, $x_{\text{RO}}(t)$ and $x_{\text{MU}}(t)$ which will be used in transmissions in the radar only sub-channel and mixed use sub-channel respectively. Since $X(f)$ is spectrally flat, this implies that both $X_{\text{RO}}(f)$ and $X_{\text{MU}}(f)$ are spectrally flat as well. This partitioning in the frequency domain also makes the two signals orthogonal in frequency. Additionally, the two signals have the following property as well

$$x_{\text{RO}}(t) + x_{\text{MU}}(t) = x(t). \quad (6.27)$$

Thus, after transmission, the radar receiver will observe the following return signal

$$\begin{aligned} z(t) &= [a x_{\text{RO}}(t - \tau) + n_{\text{RO}}(t)] \\ &\quad + [a x_{\text{MU}}(t - \tau) + n_{\text{MU}}(t) + b r(t)], \end{aligned}$$

where $r(t)$ is the communications signal that is present in the mixed use channel, $n_{\text{RO}}(t) \sim \mathcal{CN}(0, \alpha\sigma^2)$ is complex AWGN in the radar only sub-channel and $n_{\text{MU}}(t) \sim \mathcal{CN}(0, (1 - \alpha)\sigma^2)$ is complex AWGN in the mixed use sub-channel and $\sigma^2 = k_B / T_{\text{temp}} B$ is the variance of additive white gaussian noise in a channel that was the sum of both sub channels. Using the property of addition of two gaussian random processes and the property described in equation (6.27), we get

$$z(t) = a x(t - \tau) + b r(t) + n(t). \quad (6.28)$$

Using this return signal, we will derive the Cramer-Rao lower bound on the variance for joint time delay-phase estimation. Let $\theta = \tau$ be the parameter to be estimated. From equation (6.28), we see that $z(t) \sim \mathcal{CN}(x(t - \tau) + r(t), \sigma^2)$ and has the following probability density function,

$$p(z(t); \theta) = \frac{1}{\pi\sigma^2} e^{-\frac{\|z(t) - a x(t - \tau) - b r(t)\|^2}{\sigma^2}}. \quad (6.29)$$

The corresponding log-likelihood function is given by

$$\log p(z(t); \theta) = -\log(\pi\sigma^2) - \frac{\|z(t) - a x(t - \tau) - b r(t)\|^2}{\sigma^2} \quad (6.30)$$

and the score function, $s(\theta; z(t))$ is given by

$$s(\theta; z(t)) = \frac{\partial}{\partial \theta} \{\log p(z(t); \theta)\} = \frac{n^*(t) a x'(t - \tau)}{\sigma^2} + c.c. \quad (6.31)$$

where c.c. stands for complex conjugate term and $x'(t - \tau) = \frac{\partial}{\partial \tau} x(t - \tau)$. Now, the Fisher information for this estimation problem, J , is given by

$$\begin{aligned} J &= \langle s(\theta; z(t)) s^*(\theta; z(t)) \rangle \\ &= \\ &\left\langle \left(\frac{n^*(t) a x'(t - \tau)}{\sigma^2} + c.c. \right) \left(\frac{[a^* x'(t - \tau)]^* n(t)}{\sigma^2} + c.c.^* \right) \right\rangle \end{aligned}$$

On simplification, we see that

$$J = 2 \left\langle \frac{\|a\|^2 n(t)n^*(t)x'(t-\tau)[x'(t-\tau)]^*}{\sigma^4} \right\rangle \quad (6.32)$$

where the cross-terms in the product become 0 due to $\langle n(t) \rangle = 0$ and the independence of $x(t-\tau)$ and $n(t)$. The factor of two comes from the complex conjugate term. Using the fact that $\langle n(t)n^*(t) \rangle = \sigma^2$ and simplifying, we see that

$$\begin{aligned} J &= \frac{2\|a\|^2 \langle x'(t-\tau)[x'(t-\tau)]^* \rangle}{\sigma^2} \\ &= \frac{2\|a\|^2 \|x'_{\text{RO}}(t-\tau) + x'_{\text{MU}}(t-\tau)\|^2}{\sigma^2} \end{aligned}$$

By multiplying the terms out, converting to frequency domain and applying Parseval's Theorem, the time-shift and differentiation properties of the Fourier Transform and the orthogonality of $X_{\text{RO}}(f)$ and $X_{\text{MU}}(f)$, for spectrally flat $X_{\text{RO}}(f)$ and $X_{\text{MU}}(f)$, we get

$$\begin{aligned} J &= \frac{2\|a\|^2}{\sigma^2} \left[\int_{B_O - \frac{B}{2}}^{B_O - \frac{B}{2} + \alpha B} df (2\pi f)^2 \langle X_{\text{RO}}(f) X_{\text{RO}}^*(f) \rangle \right. \\ &\quad \left. + \int_{B_O + \frac{B}{2}}^{B_O - \frac{B}{2} + \alpha B} df (2\pi f)^2 \langle X_{\text{MU}}(f) X_{\text{MU}}^*(f) \rangle \right] \\ &= \frac{2}{\sigma^2} \left[\frac{4\pi^2 \|a\|^2 \alpha T B \rho_{\text{RO}}}{3} f^3 \Big|_{B_O - \frac{B}{2}}^{B_O - \frac{B}{2} + \alpha B} \right. \\ &\quad \left. + \frac{4\pi^2 \|a\|^2 (1-\alpha) T B \rho_{\text{MU}}}{3} f^3 \Big|_{B_O - \frac{B}{2} + \alpha B}^{B_O + \frac{B}{2}} \right] \end{aligned}$$

to finally get

$$\begin{aligned} J &= \frac{8\pi^2 \|a\|^2 \alpha T B \rho_{\text{RO}}}{3k_B T_{\text{temp}} B} \left[\left(B_O - \frac{B}{2} + \alpha B \right)^3 - \left(B_O - \frac{B}{2} \right)^3 \right] \\ &\quad + \frac{8\pi^2 \|a\|^2 (1-\alpha) T B \rho_{\text{MU}}}{3k_B T_{\text{temp}} B} \\ &\quad \cdot \left[\left(B_O + \frac{B}{2} \right)^3 - \left(B_O - \frac{B}{2} + \alpha B \right)^3 \right]. \end{aligned} \quad (6.33)$$

We consider B_O to be a free parameter. We select a value of B_O by looking at the reduced Fisher information [23, 27] for time-delay estimation derived from the Fisher information matrix of joint amplitude and time-delay estimation. We set the value of B_O such that the regular Fisher information for time-delay estimation, given by Equation (6.33), and the reduced Fisher information for time delay estimation will be equal. In general, the reduced Fisher information is given by Equation (B.15). As shown in Appendix B, the resultant value for B_O is given by

$$B_O = \frac{\alpha B (\alpha - 1) [\rho_{\text{MU}}(\alpha - 1) + \rho_{\text{RO}}\alpha]}{2(\rho_{\text{MU}}(\alpha - 1)^2 + \rho_{\text{RO}}\alpha^2)}. \quad (6.34)$$

From equation (6.25), we see that,

$$\rho_{\text{RO}} = \frac{P_{\text{rad}} - (1 - \alpha)B \rho_{\text{MU}}}{\alpha B} \quad (6.35)$$

$$\rho_{\text{MU}} = \frac{P_{\text{rad}} - \alpha B \rho_{\text{RO}}}{(1 - \alpha)B}. \quad (6.36)$$

The value of the power spectral density utilized by the radar only sub-band, ρ_{RO} , that maximizes the Fisher information for a time-delay estimator is obtained by plugging in Equations (6.34) and (6.36) into J and taking it's derivative with respect to ρ_{RO} , setting the resultant equation to 0 and solving for ρ_{RO} . ρ_{MU} is obtained in a similar way, except that equation (6.35) is used in J instead of equation (6.36). ρ_{RO} and ρ_{MU} are given by the following equations,

$$\begin{aligned} \rho_{\text{RO}} = & \frac{P_{\text{rad}}\alpha(4\alpha^5 - 12\alpha^4 + 20\alpha^3 - 20\alpha^2 + 9\alpha - 1)}{B \alpha^2 Q} \\ & - \frac{\sqrt{3P_{\text{rad}}^2(\alpha^3 - \alpha^2)^2(-4\alpha^4 + 8\alpha^3 - 12\alpha^2 + 8\alpha - 1)}}{b \alpha^2 Q} \end{aligned} \quad (6.37)$$

$$\begin{aligned} \rho_{\text{MU}} = & \frac{\sqrt{3P_{\text{rad}}^2(\alpha^3 - \alpha^2)^2(-4\alpha^4 + 8\alpha^3 - 12\alpha^2 + 8\alpha - 1)}}{B (\alpha - 1)^2 Q} \\ & + \frac{P_{\text{rad}}\alpha(-4\alpha^5 + 12\alpha^4 - 20\alpha^3 + 20\alpha^2 - 9\alpha + 1)}{B (\alpha - 1)^2 Q}, \end{aligned} \quad (6.38)$$

where

$$Q = (8\alpha^5 - 20\alpha^4 + 32\alpha^3 - 28\alpha^2 + 10\alpha - 1).$$

The resultant estimation rate bound for the radar System in both sub-channels is given by

$$\begin{aligned} R_{\text{est}} &\leq B \log_2 \left[1 + \frac{\sigma_{\text{proc}}^2}{\sigma_{\text{est}}^2} \right]^{\frac{\delta}{TB}} \\ &= B \log_2 [1 + \sigma_{\text{proc}}^2 J]^{\frac{\delta}{TB}} \end{aligned} \quad (6.39)$$

where σ_{est}^2 is the variance of the time-delay estimation given by $\sigma_{\text{est}}^2 = J^{-1}$ and J is given by Equation (??). The corresponding communications rate bound in the mixed use channel is

$$\begin{aligned} R_{\text{com,MU}} &\leq B_{\text{mix}} \log_2 \left[1 + \frac{b^2 P_{\text{com}}}{\sigma_{\text{int+n}}^2} \right] \\ &= (1 - \alpha) B \log_2 \left[1 + \frac{b^2 P_{\text{com}}}{\sigma_{\text{int+n}}^2} \right] \end{aligned} \quad (6.40)$$

$$\begin{aligned} \sigma_{\text{int+n}}^2 &= \|a\|^2 (1 - \alpha) B \rho_{\text{MU}} \gamma^2 (1 - \alpha)^2 B^2 \sigma_{\text{proc}}^2 \\ &\quad + (1 - \alpha) k_B T_{\text{temp}} B. \end{aligned}$$

6.5 Examples

In Figures 6.5, we display an example of outer and inner bounds on performance. The parameters used in the example are displayed in Table 6.1. It is assumed that the communications system is received through an antenna sidelobe, so that the radar and communications receive gain are not identical.

In general, the inner bound is produced by the convex hull of all contributing inner bounds. According to [26, p. 3], the convex hull for a finite set P of n points can be visualized as follows

Imagine that the points are nails sticking out of the plane, take an elastic rubber band, hold it around the nails, and let it go. It will snap

around the nails, minimizing its length. The area enclosed by the rubber band is the convex hull of P.

For the optimal fisher information bound, while optimizing the distribution of radar power between the two sub-channels, it was found that the power becomes complex for $\alpha < 0.19$ and $\alpha > 0.81$. In order to get a inner-bound on rate over all values of α , the power in each sub-channel has been set linearly for $\alpha < 0.19$ and $\alpha > 0.81$ such that the total power used by both sub-channels at α value is always the total radar power, P_{rad} . Using the parameters given in Table 6.1, we get a power distribtuion as shown in Figure 6.4. We get similar power distributions for the parameters given in Tables 6.2 and 6.3.

Additional inner bounds constructed using parameters given in Tables 6.2 and 6.3 are shown in Figures 6.6 and 6.7.

In Figures 6.5-6.7, we indicate an outer bound in red. We indicate the convex hull of all inner bounds in purple. We indicate in green, the bound on successive interference cancellation (SIC), presented in Equation (6.6). The best case system performance given SIC is at the vertex (at the intersection of the green and red lines), which is determined by the joint solution of Equations (6.6) and (5.1). The inner bound that linearly interpolates between this vertex and the radar-free communications bound in Equation (6.5) is indicated by the gray dashed line. The water-filling bound is indicated by the blue line. The water-filling bound is not guaranteed to be convex. The water-filling bound is not guaranteed to be greater than the linearly interpolated bound. The isolated sub-band inner bound is indicated by the brown line and the optimal fisher information bound is indicated by the black line.

In the example, we see that the water-filling bound exceeds the linearly interpolated bound and all other inner bounds, that the optimal fisher information bound is always lower than the water-filling bound and can either exceed both the isolated

sub-band bound and the linearly interpolated bounds, exceed the isolated sub-band bound only or be lower than both the linearly interpolated bound and the isolated sub-band bound depending on the value of α used. We also very clearly see that the isolated sub-band inner bound and the water-filling bound deviate after the critical point is reached.

Table 6.1: Parameters for Example Performance Bound #1

Parameter	Value
Bandwidth	5 MHz
Center Frequency	3 GHz
Temperature	1000 K
Communications Range	10 km
Communications Power	300 mW
Communications Antenna Gain	0 dBi
Radar Target Range	200 km
Radar Antenna Gain	30 dBi
Radar Power	100 kW
Target Cross Section	10 m ²
Target Process Standard Deviation	50 m
Time-Bandwidth Product	100
Radar duty factor	0.01

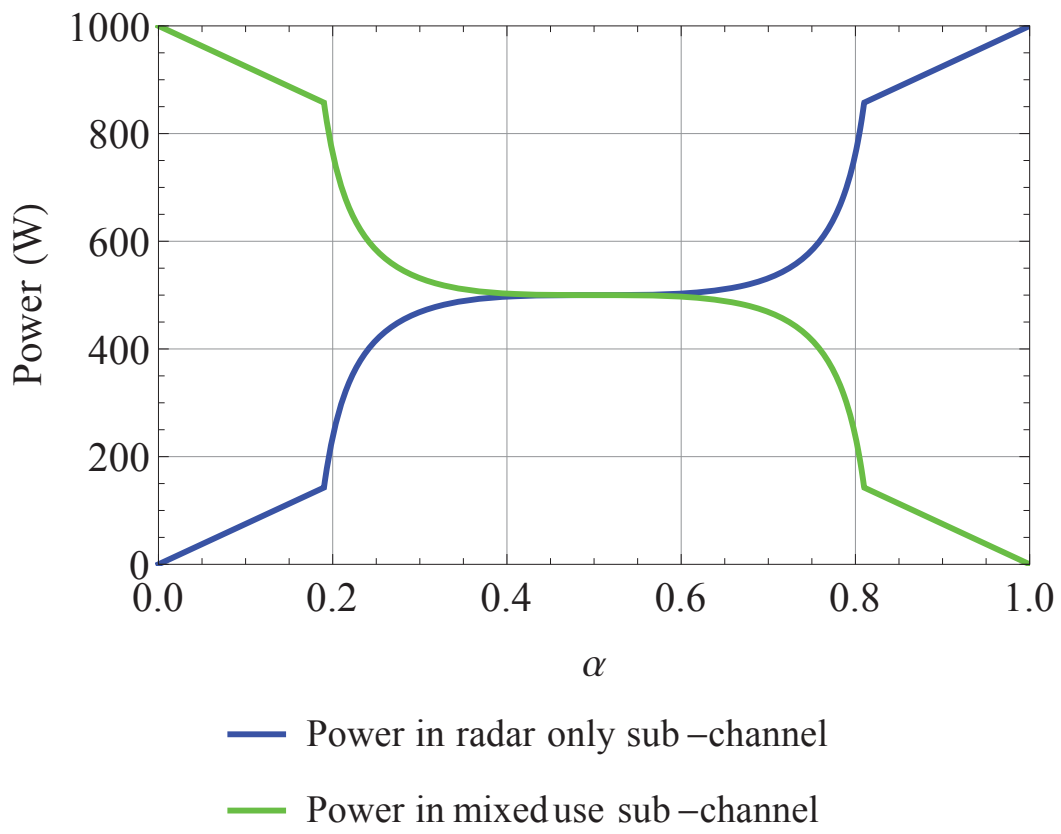


Figure 6.4: Power distribution vs. (α) for Optimal Fisher Information Bound.

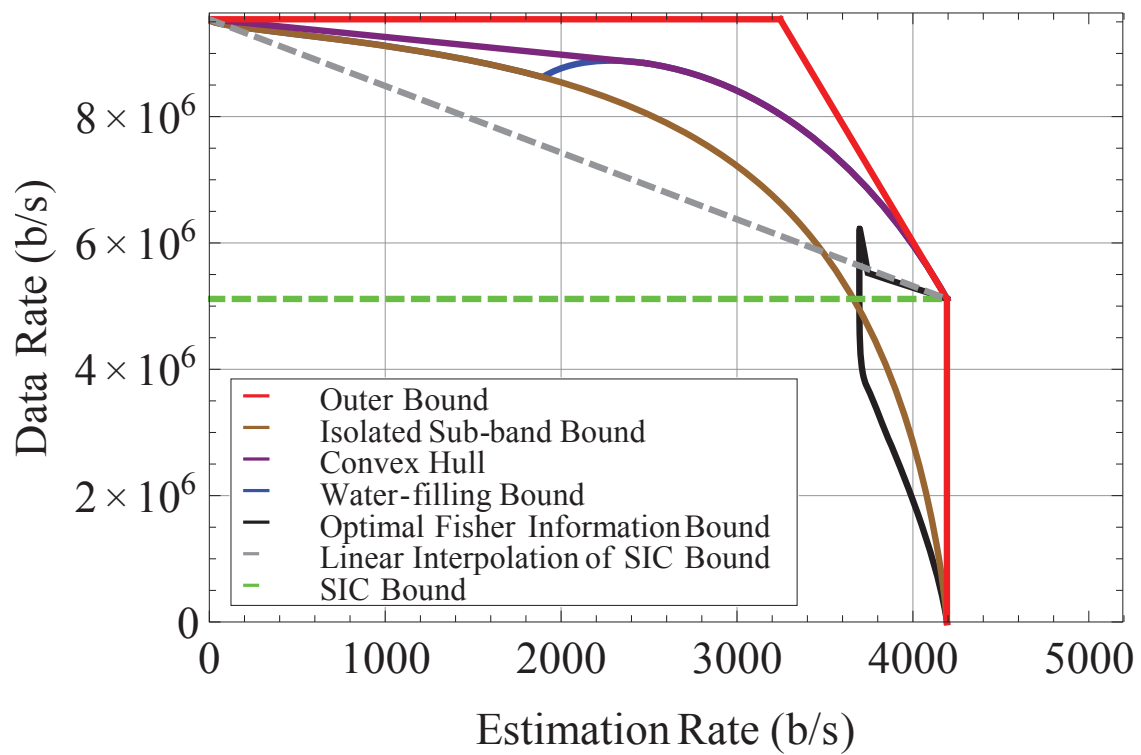


Figure 6.5: Data Rate and Estimation Rate Bounds for Parameters in Table 6.1.

Table 6.2: Parameters for Example Performance Bound #2

Parameter	Value
Bandwidth	10 MHz
Center Frequency	3 GHz
Temperature	1000 K
Communications Range	50 km
Communications Power	1 W
Communications Antenna Gain	0 dBi
Radar Target Range	60 km
Radar Antenna Gain	30 dBi
Radar Power	0.5 kW
Target Cross Section	10 m ²
Target Process Standard Deviation	80 m
Time-Bandwidth Product	200
Radar duty factor	0.05

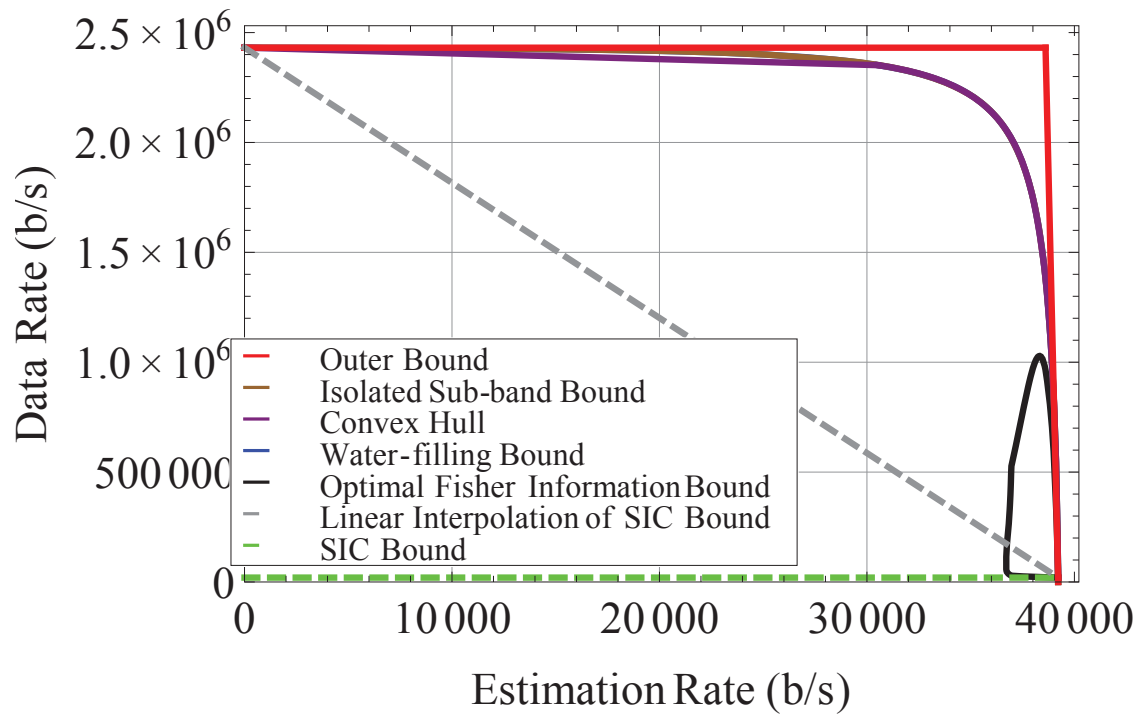


Figure 6.6: Data Rate and Estimation Rate Bounds for Parameters in Table 6.2.

Table 6.3: Parameters for Example Performance Bound #3

Parameter	Value
Bandwidth	5 MHz
Center Frequency	3 GHz
Temperature	1000 K
Communications Range	10 km
Communications Power	100 mW
Communications Antenna Gain	0 dBi
Radar Target Range	150 km
Radar Antenna Gain	30 dBi
Radar Power	100 kW
Target Cross Section	10 m ²
Target Process Standard Deviation	100 m
Time-Bandwidth Product	10
Radar duty factor	0.01

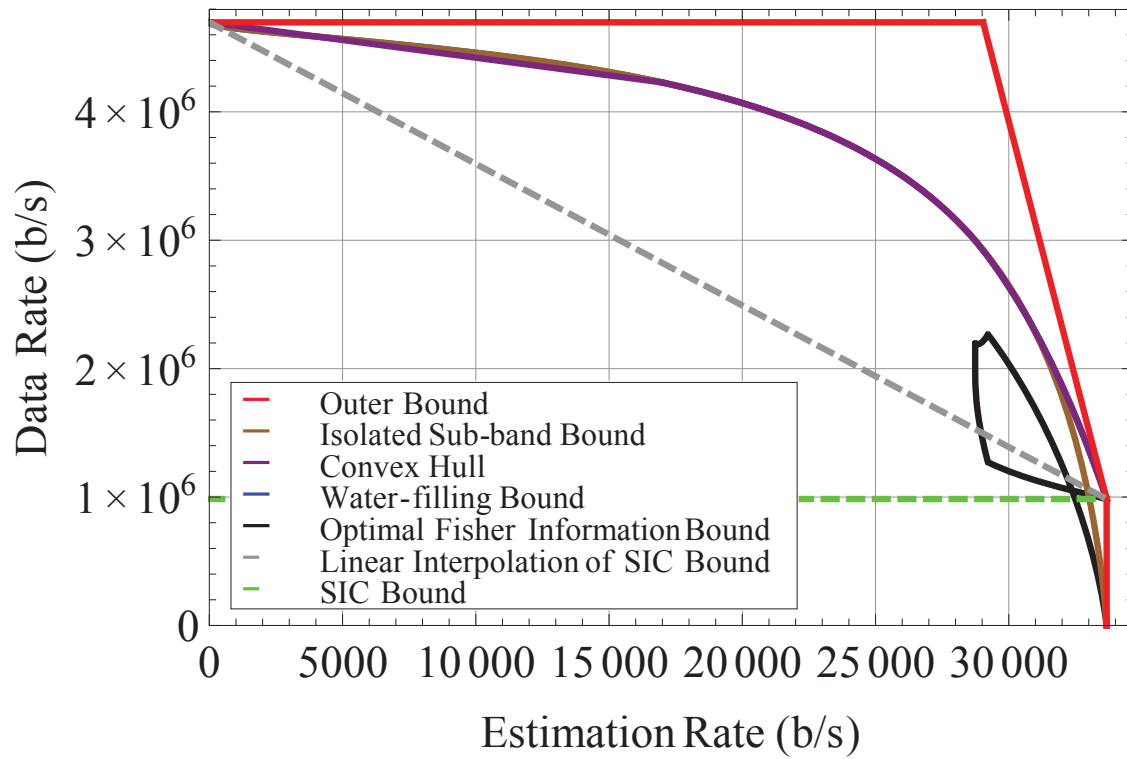


Figure 6.7: Data Rate and Estimation Rate Bounds for Parameters in Table 6.3.

Chapter 7

CONCLUSION

7.1 Summary

In this thesis, we provided a novel approach for producing joint radar-communications performance bounds. We first developed a unique joint receiver signal model similar to the communication multiple access channel which enabled us to consider many novel approaches to designing a joint radar-communications system. In order to analyze the performance of the joint receiver in terms of information rates, we needed to derive a metric analogous to the data information rate of a communication system. This was done in Chapter 4, where we went about developing such a metric, called the radar estimation information rate, by using the concept of mutual information between the estimation parameter and the estimation (process) uncertainty of that parameter. The performance for the various joint systems we considered were then evaluated in terms of the data rate and the estimation rate.

We derive the SIC inner bound by considering a joint system in which both systems occupy the same frequency band and we vary both the data rate and the estimation rate such that at one extreme the estimation rate is almost zero and the data rate is the capacity of the channel to the other extreme where the data rate is sufficiently low that the communications signal can be successfully decoded and removed from the underlying received signal, thereby removing any interference in estimating the radar parameter. We also derive the isolated sub-band inner bound by considering a joint system in which the communications system and the radar system both occupy different sub-channels with different frequencies and then the total power of each

system is utilized completely in each respective sub-band. This implies that there is no interference between either systems. Furthermore, we derive the communications water-filling inner bound by considering a joint system in which the communications system bandwidth is split across two sub-channels with different frequencies and then the total communications power is split across the two sub-bands by using the water-filling algorithm. Finally, we derive the optimal Fisher information inner bound by considering a joint system in which the radar system bandwidth is split across two sub-channels with different frequencies and then the total communications power is split across the two sub-bands in such a way that the fisher information of the time-delay estimator is maximized (Cramer-Rao lower bound is minimized).

Given a set of parameters and constraints on the radar and communication systems, we can use the derived inner bounds to design appropriate joint systems. In the case where we have full control over all parameters for both systems, we can simply derive all the inner bounds and calculate the convex hull of all inner bounds. This gives a complete profile of all possible data and estimation rates for the joint system. Depending on the requirements of the system, we can choose which region to operate in, thus also choosing the algorithm that will be implemented by the system.

In the case where we have no control over some of a system's parameters, we can design a joint system based on just an appropriate subset of the derived inner bounds. By choosing an appropriate subset of inner bounds and taking the convex hull of the contributing inner bounds, a unique profile of all possible data and estimation rates is developed. We can then choose which region to operate in, depending on the requirements of the system, thus also choosing the algorithm that will be implemented by the system. An example would be that if in a certain channel there is a communications system (over which we have no control) that occupies the a part or the entire bandwidth and we need to design a radar system that can coexist with the communi-

cations system, we could decide that either the SIC algorithm or a set containing the optimal fisher information algorithm and the isolated sub-band algorithm would be the most appropriate algorithm to implement (depending on how much bandwidth is occupied by communications). We then take the convex hull of all contributing inner bounds (SIC or set of optimal fisher information and isolated sub-band) and develop a unique profile of all possible data and estimation rates for the given constraints.

7.2 Future Research

We intend on applying the concepts presented in this thesis to a joint radar-communications system where the radar system being utilized is a continuous wave (CW) radar and re deriving all the inner bounds on performance. CW radars are simplistic in design and can be highly accurate. They also can potentially reduce the required radar bandwidth significantly [28]. CW radars can also through Doppler processing, increase the detection range with out increasing the radar transmit power. It is due to all these advantages that we intend on designing a joint system utilizing a CW radar.

We also intend on designing joint radar-communications systems in which the radar system estimates the amplitude (Cross Section) of the target along with the time delay. In this thesis, we have assumed that the target amplitude is known. Furthermore, we intend on adding a target tracking algorithm to the radar system (using Kalman filters) instead of assuming that the target range is always known up to some underlying target range uncertainty.

REFERENCES

- [1] D.W. Bliss. Cooperative radar and communications signaling: the estimation and information theory odd couple. *IEEE Interantional Radar Conference*, 2014.
- [2] P.M. Woodward and I.L. Davies. A theory of radar information. *Philosophical Magazine Series 7*, 41(321):1001–1017, 1993.
- [3] P.M. Woodward. Information theory and the design of radar receivers. *Proceedings of the IRE*, 39(12):1521–1524, Dec. 1993.
- [4] Philip M. Woodward. *Probability and Information Theory: With Applications to Radar*. Artech House, Incorporated, 1953.
- [5] P.M. Woodward. Radar ambiguity analysis. *RRE Technical Note*, (731), Feb. 1967.
- [6] M.R. Bell. Information theory and radar waveform design. *IEEE Transactions on Information Theory*, 39(5):1578–1597, Sep. 1993.
- [7] S.U. Pillai, H.S. Oh, D.C. Youla, and J.R. Guerci. Optimal transmit-receiver design in the presence of signal-dependent interference and channel noise. *IEEE Transactions on Information Theory*, 46(2):577–584, Mar. 2000.
- [8] D.A. Garren, M.K. Osborn, A.C. Odom, J.S. Goldstein, S.U. Pillai, and J.R. Guerci. Enhanced target detection and identification via optimised radar transmission pulse shape. *IEE Proceedings on Radar, Sonar and Navigation*, 148(3):130–138, Jun. 2001.
- [9] L. S. Wang, J. P. McGeehan, C. Williams, and A. Doufexi. Application of cooperative sensing in radar-communications coexistence. *IET Communications*, 2(6):856–868, July 2008.
- [10] S. S. Bhat, R. M. Narayanan, and M. Rangaswamy. Bandwidth sharing and scheduling for multimodal radar with communications and tracking. In *IEEE Sensor Array and Multichannel Signal Processing Workshop*, pages 233–236, June 2012.
- [11] H. Deng and B. Himed. Interference mitigation processing for spectrum-sharing between radar and wireless communications systems. *IEEE Transactions on Aerospace and Electronic Systems*, 49(3):1911–1919, Jul. 2013.
- [12] A. Babaei, W.H. Tranter, and T. Bose. A practical precoding approach for radar/communications spectrum sharing. *International Conference on Cognitive Radio Oriented Wireless Networks*, pages 13–18, Jul. 2013.
- [13] S. Sodagari, A. Khawar, T. Clancy, and R. McGwier. A projection-based approach for radar and telecommunication systems coexistence. In *IEEE Global Communincations Conference*, pages 5232–5236, December 2012.

- [14] D. Garmatyuk, Y.J. Morton, and X. Mao. On co-existence of in-band uwb-ofdm and gps signals: Tracking performance analysis. *IEEE/ION Position, Location and Navigation Symposium*, pages 196–202, May 2008.
- [15] S.D. Blunt, P. Yatham, and J. Stiles. Intrapulse radar-embedded communications. *IEEE Transactions on Aerospace and Electronic Systems*, 46(3):1185–1200, Jul. 2010.
- [16] S. Gogineni, M. Rangaswamy, and A. Nehorai. Multi-modal ofdm waveform design. *IEEE Radar Conference*, pages 1–5, May 2013.
- [17] D. Garmatyuk, J. Schuerger, K. Kauffman, and S. Spalding. Wideband ofdm system for radar and communications. *IEEE Vehicular Technology Conference*, pages 1–6, May 2009.
- [18] P.C. Mahalanobis. On the generalised distance in statistics. *Proceedings of the National Institute of Sciences of India*, 2(1):49–55, Apr. 1936.
- [19] M. Roberton and E.R. Brown. Integrated radar and communications based on chirped spread-spectrum techniques. *IEEE MTT-S International Microwave Symposium Digest*, 1:611–614, Jun. 2003.
- [20] B. J. Donnet and I. D. Longstaff. Combining MIMO radar with OFDM communications. *Proceedings of the 3rd European Radar Conference*, pages 37–40, Sept. 2006.
- [21] C. Sturm, T. Zwick, and W. Wiesbeck. An ofdm system concept for joint radar and communications operations. *IEEE Vehicular Technology Conference*, pages 1–5, April 2009.
- [22] C. Sturm and W. Wiesbeck. Waveform design and signal processing aspects for fusion of wireless communications and radar sensing. *Proceedings of the IEEE*, 99(7):1236–1259, Jul. 2011.
- [23] Daniel W. Bliss and Siddhartan Govindasamy. *Adaptive Wireless Communications: MIMO Channels and Networks*. Cambridge University Press, 2013.
- [24] Mark A. Richards, James A. Scheer, and William A. Holm. *Principles of Modern Radar: Basic Principles*. SciTech Publishing, 2010.
- [25] T. M. Cover and J. A. Thomas. *Elements of Information Theory, 2nd Edition*. John Wiley & Sons, New York, 2006.
- [26] Mark de Berg, Cheong Otfried, Mark van Kreveld, and Mark Overmars. *Computational Geometry: Algorithms and Applications, 3rd Edition*. Springer, 2008.
- [27] D. F. Delong. Multiple signal direction finding with thinned linear arrays. Technical Report TST-68, DTIC:ADA128924, MIT Lincoln Laboratory, April 1983.

- [28] C.A. Jackson, J.R. Holloway, R. Pollard, R. Larson, C. Sarno, C. Baker, K. Woodbridge, R.F. Ormondroyd, M.B. Lewis, and A.G. Stove. Spectrally efficient radar systems in the l and s bands. *IET International Conference on Radar Systems*, pages 1–6, Oct. 2007.

APPENDIX A
DERIVATION OF CRAMER-RAO LOWER BOUND FOR TIME-DELAY
ESTIMATION

APPENDIX A

DERIVATION OF CRAMER-RAO LOWER BOUND FOR TIME-DELAY ESTIMATION

In this chapter, we will be deriving the Cramer-Rao Lower bound on time-delay estimation on a SISO (single-input single-output) channel with circularly symmetric Gaussian noise [24]. The Cramer-Rao bound gives the best performance (in terms of variance of error) of an unbiased estimator.

We assume that the received signal of the time-delay estimator is given by

$$z(t) = a x(t - \tau) + n(t), \quad (\text{A.1})$$

where $x(t)$ is the transmitted signal whose frequency representation, $X(f)$ has full bandwidth B , $x(t - \tau)$ is the delayed version of the transmitted signal, a is the combined radar cross-section, antenna and propagation gain and $n(t)$ is circularly symmetric Gaussian noise with zero mean and variance σ^2 .

Let $\theta = \tau$ be the parameter to be estimated. From equation (A.1), we see that $z(t) \sim \mathcal{CN}(x(t - \tau), \sigma^2)$ and has the following probability density function,

$$p(z(t); \theta) = \frac{1}{\pi\sigma^2} e^{-\frac{\|z(t) - a x(t - \tau)\|^2}{\sigma^2}}. \quad (\text{A.2})$$

The corresponding log-likelihood function is given by

$$\log p(z(t); \theta) = -\log(\pi\sigma^2) - \frac{\|z(t) - a x(t - \tau)\|^2}{\sigma^2} \quad (\text{A.3})$$

and the score function, $s(\theta; z(t))$ is given by

$$s(\theta; z(t)) = \frac{\partial}{\partial \theta} \{\log p(z(t); \theta)\} = \frac{a n^*(t) x'(t - \tau)}{\sigma^2} + c.c. \quad (\text{A.4})$$

where c.c. stands for complex conjugate term and $x'(t - \tau) = \frac{\partial}{\partial \tau} x(t - \tau)$. Now, the Fisher information for this estimation problem, J , is given by

$$\begin{aligned} J &= \langle s(\theta; z(t)) s^*(\theta; z(t)) \rangle \\ &= \left\langle \left(\frac{n^*(t) a x'(t - \tau)}{\sigma^2} + c.c. \right) \left(\frac{a^* [x'(t - \tau)]^* n(t)}{\sigma^2} + c.c.^* \right) \right\rangle \end{aligned}$$

On simplification, we see that

$$J = 2 \left\langle \frac{\|a\|^2 n(t) n^*(t) x'(t - \tau) [x'(t - \tau)]^*}{\sigma^4} \right\rangle \quad (\text{A.5})$$

where the cross-terms in the product become 0 due to $\langle n(t) \rangle = 0$ and the independence of $x(t-\tau)$ and $n(t)$. The factor of two comes from the complex conjugate term. Using the fact that $\langle n(t)n^*(t) \rangle = \sigma^2$ and simplifying, we see that

$$J = \frac{2\|a\|^2 \langle x'(t-\tau)[x'(t-\tau)]^* \rangle}{\sigma^2} \quad (\text{A.6})$$

By converting to frequency domain and applying Parseval's Theorem and the time-shift and differentiation properties of the Fourier Transform, we get

$$\begin{aligned} J &= \frac{2\|a\|^2}{\sigma^2} \left[\int_{-\frac{B}{2}}^{\frac{B}{2}} df (2\pi f)^2 \langle X(f)X^*(f) \rangle \right] \\ &= \frac{2}{\sigma^2} \left[\frac{4\pi^2\|a\|^2 TP_{\text{rad}}}{3} f^3 \Big|_{-\frac{B}{2}}^{\frac{B}{2}} \right] \end{aligned} \quad (\text{A.7})$$

to finally get

$$\begin{aligned} J &= \frac{8\pi^2\|a\|^2 TP_{\text{rad}} B^2}{12k_B T_{\text{temp}} B} \\ &= 2 \left(\frac{(2\pi)^2 \|a\|^2 TP_{\text{rad}} B^2}{12k_B T_{\text{temp}} B} \right) \\ &= 2 \left(\frac{(2\pi)^2 (B_{\text{rms}}^2 \|a\|^2 TP_{\text{rad}})}{\sigma^2} \right) \\ &= 2 \left((2\pi)^2 B_{\text{rms}}^2 \text{ISNR} \right), \end{aligned} \quad (\text{A.8})$$

where ISNR stands for integrated SNR, and $\gamma^2 = (2\pi^2)/12$ is the scaling constant for a flat spectral shape and by centering the spectrum at an appropriate point(i.e. choosing the origin of the spectrum), we get the RMS bandwidth B_{rms} .

Thus, the Cramer-Rao lower bound for time delay estimation, $\sigma_{\tau;\text{est}}^2$ is given by

$$\sigma_{\tau;\text{est}}^2 = J^{-1} = \left(\frac{1}{8\pi^2 B_{\text{rms}}^2 \text{ISNR}} \right). \quad (\text{A.9})$$

APPENDIX B
DERIVATION OF FISHER INFORMATION CROSS TERMS FOR JOINT
AMPLITUDE AND TIME-DELAY ESTIMATION

APPENDIX B

DERIVATION OF REDUCED FISHER INFORMATION FOR TIME-DELAY ESTIMATION FROM FISHER INFORMATION MATRIX FOR JOINT AMPLITUDE AND TIME-DELAY ESTIMATION

In this chapter, we will first derive the fisher information cross terms for joint amplitude and time-delay estimation and find the value of the free parameter B_O that sets these cross-terms to 0. We will then show that by setting the cross-terms to 0, the reduced fisher information for time-delay estimation is the same as the Fisher information for time-delay estimation, given by Equation (6.33).

We consider the same scenario as described in Section 6.4. The total bandwidth is split into two sub-bands and the radar power (or power spectral density) is distributed between the two sub-bands. The bandwidth will be split between the two sub-bands according to some α such that,

$$\begin{aligned} B &= B_{\text{rad}} + B_{\text{mix}} & (\text{B.1}) \\ B_{\text{rad}} &= \alpha B \\ B_{\text{mix}} &= (1 - \alpha) B, \end{aligned}$$

and the power spectral densities, ρ_{RO} and ρ_{MU} , utilized by the radar only and mixed use sub-bands respectively, will be split according to the same α ,

$$P_{\text{rad}} = P_{\text{rad,rad}} + P_{\text{rad,mix}} \quad (\text{B.2})$$

$$\begin{aligned} P_{\text{rad,rad}} &= B_{\text{rad}} \rho_{\text{RO}} \\ &= \alpha B \rho_{\text{RO}} \end{aligned} \quad (\text{B.3})$$

$$\begin{aligned} P_{\text{rad,mix}} &= B_{\text{mix}} \rho_{\text{MU}} \\ &= (1 - \alpha) B \rho_{\text{MU}}. \end{aligned} \quad (\text{B.4})$$

We will have the following constraints on power and energy of the radar system in the two sub-channels,

$$P_{\text{rad}} = \alpha B \rho_{\text{RO}} + (1 - \alpha) B \rho_{\text{MU}} \quad (\text{B.5})$$

$$E_{\text{rad}} = T P_{\text{rad}} = \alpha T B \rho_{\text{RO}} + (1 - \alpha) T B \rho_{\text{MU}}. \quad (\text{B.6})$$

Now, consider a radar signal $x(t)$ with bandwidth B , whose frequency spectrum $X(f)$ is centered around B_O . We assume that $X(f)$ is spectrally flat. We will now partition the frequency spectrum into two portions, $X_{\text{RO}}(f)$ and $X_{\text{MU}}(f)$ with bandwidths αB and $(1 - \alpha)B$ respectively, thereby creating two new signals, $x_{\text{RO}}(t)$ and $x_{\text{MU}}(t)$ which will be used in transmissions in the radar only sub-channel and mixed use sub-channel respectively. Since $X(f)$ is spectrally flat, this implies that

both $X_{\text{RO}}(f)$ and $X_{\text{MU}}(f)$ are spectrally flat as well. This partitioning in the frequency domain also makes the two signals orthogonal in frequency. Additionally, the two signals have the following property as well

$$x_{\text{RO}}(t) + x_{\text{MU}}(t) = x(t). \quad (\text{B.7})$$

Thus, after transmission, the radar receiver will observe the following return signal

$$z(t) = [a x_{\text{RO}}(t - \tau) + n_{\text{RO}}(t)] \\ + [a x_{\text{MU}}(t - \tau) + n_{\text{MU}}(t) + b r(t)],$$

where $r(t)$ is the communications signal that is present in the mixed use channel, $n_{\text{RO}}(t) \sim \mathcal{CN}(0, \alpha\sigma^2)$ is complex AWGN in the radar only sub-channel and $n_{\text{MU}}(t) \sim \mathcal{CN}(0, (1 - \alpha)\sigma^2)$ is complex AWGN in the mixed use sub-channel and $\sigma^2 = k_B / T_{\text{temp}}$ B is the variance of additive white gaussian noise in a channel that was the sum of both sub channels. Using the property of addition of two gaussian random processes and the property described in equation (B.7), we get

$$z(t) = a x(t - \tau) + b r(t) + n(t). \quad (\text{B.8})$$

Let $\theta = [\tau]$ be the parameters to be estimated. From equation (B.8), we see that $z(t) \sim \mathcal{CN}(x(t - \tau), \sigma^2)$ and has the following probability density function

$$p(z(t); \theta) = \frac{1}{\pi\sigma^2} e^{-\frac{\|z(t) - a x(t - \tau)\|^2}{\sigma^2}}. \quad (\text{B.9})$$

The corresponding log-likelihood function is given by

$$\log p(z(t); \theta) = -\log(\pi\sigma^2) - \frac{\|z(t) - a x(t - \tau)\|^2}{\sigma^2} \quad (\text{B.10})$$

and the score function, $s(\theta; z(t))$ is given by

$$s(\theta; z(t)) = \frac{\partial}{\partial \theta} \{\log p(z(t); \theta)\} = \begin{pmatrix} \frac{a n^*(t) x'(t - \tau)}{\sigma^2} + c.c. \\ \frac{n^*(t) x(t - \tau)}{\sigma^2} + c.c. \end{pmatrix} \quad (\text{B.11})$$

where c.c. stands for the complex conjugate term and $x'(t - \tau) = \frac{\partial}{\partial \tau} x(t - \tau)$. Now, the Fisher Information Matrix for this estimation problem, \mathbf{J} , is given by

$$\mathbf{J} = \langle s(\theta; z(t)) s^\dagger(\theta; z(t)) \rangle \\ = \left\langle \begin{pmatrix} \frac{a n^*(t) x'(t - \tau)}{\sigma^2} + c.c. \\ \frac{n^*(t) x(t - \tau)}{\sigma^2} + c.c. \end{pmatrix} \begin{pmatrix} \frac{a^* [x(t - \tau)]^* n(t)}{\sigma^2} + c.c.* & \frac{x^*(t - \tau) n(t)}{\sigma^2} + c.c.* \end{pmatrix} \right\rangle \\ = \begin{pmatrix} J_{\tau, \tau} & J_{\tau, a} \\ J_{a, \tau} & J_{a, a} \end{pmatrix},$$

where

$$\begin{aligned}
J_{\tau,\tau} &= \left\langle \left(\frac{a n^*(t) x'(t-\tau)}{\sigma^2} + \frac{a^* n(t) [x'(t-\tau)]^*}{\sigma^2} \right) \left(\frac{a^* [x'(t-\tau)]^* n(t)}{\sigma^2} + \frac{a n^*(t) x'(t-\tau)}{\sigma^2} \right) \right\rangle \\
J_{\tau,a} &= \left\langle \left(\frac{a n^*(t) x'(t-\tau)}{\sigma^2} + \frac{a^* n(t) [x'(t-\tau)]^*}{\sigma^2} \right) \left(\frac{x^*(t-\tau) n(t)}{\sigma^2} + \frac{n'(t) x(t-\tau)}{\sigma^2} \right) \right\rangle \\
J_{a,\tau} &= \left\langle \left(\frac{n^*(t) x(t-\tau)}{\sigma^2} + \frac{n(t) x^*(t-\tau)}{\sigma^2} \right) \left(\frac{a^* [x'(t-\tau)]^* n(t)}{\sigma^2} + \frac{a x'(t-\tau) n^*(t)}{\sigma^2} \right) \right\rangle \\
J_{a,a} &= \left\langle \left(\frac{n^*(t) x(t-\tau)}{\sigma^2} + \frac{n(t) x^*(t-\tau)}{\sigma^2} \right) \left(\frac{x^*(t-\tau) n(t)}{\sigma^2} + \frac{x(t-\tau) n^*(t)}{\sigma^2} \right) \right\rangle.
\end{aligned}$$

We will now simplify the cross terms of the Fisher information matrix. Starting with $J_{\tau,a}$, we see that on simplification,

$$J_{\tau,a} = \left\langle \frac{a n(t) n^*(t) x'(t-\tau) x^*(t-\tau)}{\sigma^4} \right\rangle + \left\langle \frac{a^* n(t) n^*(t) [x'(t-\tau)]^* x(t-\tau)}{\sigma^4} \right\rangle \quad (\text{B.12})$$

where the cross-terms in the product become 0 due to $\langle n(t) \rangle = 0$ and the independence of $x(t-\tau)$ and $n(t)$. Using the fact that $\langle n(t) n^*(t) \rangle = \sigma^2$ and simplifying, we see that

$$J_{\tau,a} = \frac{a \langle x'(t-\tau) x^*(t-\tau) \rangle}{\sigma^2} + \frac{a^* \langle [x'(t-\tau)]^* x(t-\tau) \rangle}{\sigma^2}$$

By multiplying the terms out, converting to frequency domain and applying Parseval's Theorem and the time-shift and differentiation properties of the Fourier Transform, for spectrally flat $X(f)$ (or $X_{\text{RO}}(f)$ and $X_{\text{MU}}(f)$), we get

$$\begin{aligned}
J_{\tau,a} &= \frac{a}{\sigma^2} \int_{B_O - \frac{B}{2}}^{B_O + \frac{B}{2}} df \langle (j2\pi f) X(f) e^{-j2\pi f \tau} [X(f) e^{-j2\pi f \tau}]^* \rangle \\
&\quad + \frac{a^*}{\sigma^2} \int_{B_O - \frac{B}{2}}^{B_O + \frac{B}{2}} df \langle [(j2\pi f) X(f) e^{-j2\pi f \tau}]^* X(f) e^{-j2\pi f \tau} \rangle \\
&= \frac{j a}{\sigma^2} \int_{B_O - \frac{B}{2}}^{B_O + \frac{B}{2}} df (2\pi f) \langle X(f) X^*(f) \rangle - \frac{j a^*}{\sigma^2} \int_{B_O - \frac{B}{2}}^{B_O + \frac{B}{2}} df (2\pi f) \langle X^*(f) X(f) \rangle \\
&= \frac{(j a - j a^*)}{\sigma^2} \int_{B_O - \frac{B}{2}}^{B_O + \frac{B}{2}} df (2\pi f) \langle X(f) X^*(f) \rangle
\end{aligned}$$

Using the property of $x(t)$ described in Equation (B.7) and simplifying, we get

$$\begin{aligned}
J_{\tau,a} &= \frac{(j a - j a^*)}{\sigma^2} \left[\int_{B_O - \frac{B}{2}}^{B_O - \frac{B}{2} + \alpha B} df(2\pi f) \langle X_{\text{RO}}(f) X_{\text{RO}}^*(f) \rangle \right. \\
&\quad \left. + \int_{B_O - \frac{B}{2} + \alpha B}^{B_O + \frac{B}{2}} df(2\pi f) \langle X_{\text{MU}}(f) X_{\text{MU}}^*(f) \rangle \right] \\
&= \frac{(j a - j a^*)}{\sigma^2} \left[\pi \alpha T B \rho_{\text{RO}} f^2 \Big|_{B_O - \frac{B}{2}}^{B_O - \frac{B}{2} + \alpha B} \right. \\
&\quad \left. + \pi (1 - \alpha) T B \rho_{\text{MU}} f^2 \Big|_{B_O - \frac{B}{2} + \alpha B}^{B_O + \frac{B}{2}} \right] \\
&= \frac{(j a - j a^*) \pi \alpha T B \rho_{\text{RO}}}{\sigma^2} \left[\left(B_O - \frac{B}{2} + \alpha B \right)^2 - \left(B_O - \frac{B}{2} \right)^2 \right] \\
&\quad + \frac{(j a - j a^*) \pi (1 - \alpha) T B \rho_{\text{MU}}}{\sigma^2} \left[\left(B_O + \frac{B}{2} \right)^3 - \left(B_O - \frac{B}{2} + \alpha B \right)^3 \right]
\end{aligned} \tag{B.13}$$

Similarly, using the same properties as mentioned above, we can simplify the other cross term in the Fisher Information Matrix to get

$$\begin{aligned}
J_{a,\tau} = J_{\tau,a} &= \frac{(j a - j a^*) \pi \alpha T B \rho_{\text{RO}}}{\sigma^2} \left[\left(B_O - \frac{B}{2} + \alpha B \right)^2 - \left(B_O - \frac{B}{2} \right)^2 \right] \\
&\quad + \frac{(j a - j a^*) \pi (1 - \alpha) T B \rho_{\text{MU}}}{\sigma^2} \left[\left(B_O + \frac{B}{2} \right)^3 - \left(B_O - \frac{B}{2} + \alpha B \right)^3 \right]
\end{aligned}$$

In order to find the value of B_O that sets the Fisher information matrix cross-terms $J_{a,\tau}$ and $J_{\tau,a}$ to 0, we set $J_{a,\tau} = J_{\tau,a} = 0$ and solve for B_O . The resultant value for B_O is

$$B_O = \frac{B (\alpha - 1) \alpha (\rho_2 (\alpha - 1) + \rho_1 \alpha)}{2(\rho_2 (\alpha - 1)^2 + \rho_1 \alpha^2)}. \tag{B.14}$$

This means that the Fisher information cross terms will be 0 whenever the value of B_O is given by Equation (B.14). In this case, the reduced Fisher Information [23, 27] for time-delay estimation is

$$\begin{aligned}
J_{\tau,\tau}^{(R)} &= (J_{\tau,\tau} - J_{\tau,a} J_{a,a}^{-1} J_{a,\tau}) \\
&= (J_{\tau,\tau} - 0) \\
&= J_{\tau,\tau}
\end{aligned} \tag{B.15}$$